Direct Current Discharge Plasma Chemical Vapor Deposition of Nanocrystalline Graphite Films on Carbon Fibers

Leyong Zeng,[†,‡] Hongyan Peng,[§] Weibiao Wang,*[,†] Yuqiang Chen,[§] Wentao Qi,[§] Da Lei,[†,‡] Jingqiu Liang,[⊥] Jialong Zhao,[†] and Xianggui Kong[†]

Key Laboratory of Excited State Processes, Changchun Institute of Optics, Fine Mechanics and Physics, Chinese Academy of Sciences, Changchun, 130033, People's Republic of China, Graduate School of Chinese Academy of Sciences, Beijing, 100049, People's Republic of China, Department of Physics, Mudanjiang Normal College, Mudanjiang, 157012, People's Republic of China, and State Key Laboratory of Applied Optics, Changchun Institute of Optics, Fine Mechanics and Physics, Chinese Academy of Sciences, Changchun 130033, People's Republic of China

Received: February 24, 2008; Revised Manuscript Received: May 9, 2008

Nanocrystalline graphite films were synthesized on carbon fibers by the direct current discharge plasma chemical vapor deposition method. The morphology and microstructure of the obtained products were characterized by scanning electron microscopy, Raman spectroscopy, and transmission and high-resolution transmission electron microscopy. The results showed that the size and thickness of graphite nanosheets were about 0.3−2 μm and 5−20 nm, respectively, and the purity and graphitization degree of the films can be improved by increasing the deposition time of graphite nanosheets. The down-shift of the G peak in Raman spectra can be attributed to the temperature differences of samples heating by laser radiation. In comparison with the products grown on silicon substrate under similar experimental parameters, carbon fiber substrate is more favorable for the deposition of graphite structure.

1. Introduction

Graphite is a widely used material that has been intensively investigated theoretically and experimentally because of its exceptional physical and chemical properties.[1–5] Both carbon nanotubes (CNTs) and various forms of graphite (graphite nanosheets, graphite nanowalls, and so on) can be good candidates for field emission displays and other nanoelectronic devices due to the excellent performance of electron emission and electron transport.[6–9] Especially, graphite thin films of nanometer thickness have been theoretically predicted to have an unconventional electronic structure of the edge of states and a possible superconducting instability.[10–12] Moreover, the high surface-to-volume ratio and sharp edge of graphite nanosheets are attractive for fuel cells, high performance capacitors, and micro- and nanoelectronic technologies.[13,14]

Recently, nanocrystalline graphite (NCG) films have been typically prepared by the chemical vapor deposition (CVD) method on a variety of substrates, such as Si, SiO_2, Al_2O_3, and different metallic substrates.[9,15–21] However, nothing has been reported about the synthesis of graphite nanosheet films on carbon fiber substrate. Synthesizing NCG films on carbon-based substrates may improve the properties and broaden the applications of graphite nanosheets. In our previous work, graphite nanosheets have been deposited on CNTs by the microwave plasma-enhanced CVD method,[22] and different carbon nanomaterials (including CNTs, submicrotubes, and other carbon nanomaterials) have also been synthesized on carbon fibers by the floating catalyst method.[23] Carbon fibers-based C/C composites have potential applications in many fields. For example, the previous reports have indicated that carbon fibers-based C/C composites could further enhance the mechanical properties of composites, and the micro- and nanocomposites could enhance the interfacial bonding between polymer and carbon fibers.[24–26] Especially, carbon fibers are electrically conductive with high porosity, and NCG films have high surface-to-volume ratio and high porosity. The NCG films grown on carbon fibers can have potential applications as electrode materials in electrochemical fields (like fuel cells, sensors, capacitors, etc), and as hydrogen storage materials and catalysts in cleaning energy sources and protecting surroundings and so forth. Furthermore, carbon fibers-based C/C composites can have some advantages in nanoelectronic device applications. First, a carbon fiber substrate has the characteristics of electrical conductivity and chemical stability, which can improve the stability of nanoelectronic devices. Second, carbon fibers and carbon nanomaterials have similar structures, which can decrease the touch resistance and is favorable for electron transport. Third, carbon fibers-based composites can simplify the fabrication process, and decrease the fabrication cost of nanoelectronic devices, because carbon fibers-based composites can be operated conveniently. It is generally known that catalyst, reactor temperature, gas species, and gas composition are essential for the CVD growth of CNTs and other carbon nanomaterials. However, because of the similar structures between the substrate and the products, the characteristics of carbon fiber substrate are also responsible for the growth of carbon nanomaterials (CNTs, graphite nanosheets, nanodiamonds, and so on), besides the experimental parameters. Therefore, it is interesting for synthesizing carbon nanomaterials on carbon-based substrates, which is helpful for understanding the interfacial transition between different carbon-based materials.

* Corresponding author. E-mail: wangwbt@126.com,wangwbt@126.com.
[†] Key Laboratory of Excited State Processes, Changchun Institute of Optics, Fine Mechanics and Physics, Chinese Academy of Sciences.
[‡] Graduate School of Chinese Academy of Sciences.
[§] Mudanjiang Normal College.
[⊥] State Key Laboratory of Applied Optics, Changchun Institute of Optics, Fine Mechanics and Physics, Chinese Academy of Sciences.

10.1021/jp801615w CCC: $40.75
Published on Web 06/28/2008

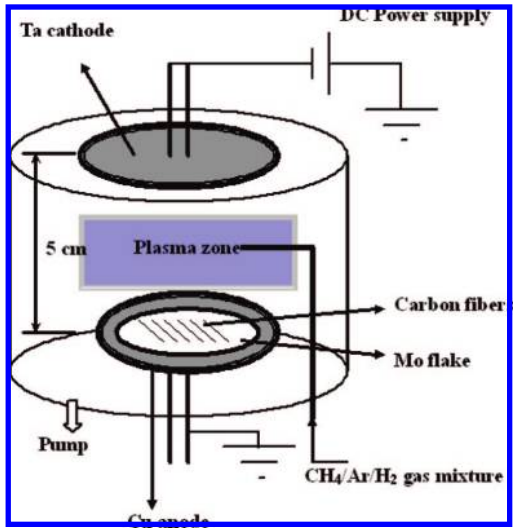

Figure 1. Schematic diagram of the DC-PCVD system for the deposition of NCG films.

In this paper, we report the preparation of NCG films on carbon fiber substrate by the direct current discharge plasma CVD (DC-PCVD) method. We study the morphology and microstructure of NCG films by scanning electron microscopy (SEM), Raman spectroscopy, transmission electron microscopy (TEM), and high-resolution transmission electron microscopy (HRTEM). Finally, we discuss the effect of carbon fiber substrate on the deposition of NCG films, compared with the products grown on silicon substrate under similar experimental conditions.

2. Experimental Section

The schematic diagram of the DC-PCVD system for the deposition of NCG films is shown in Figure 1. The Ta cathode was linked with a high-voltage DC power supply, and the Cu anode was connected with the ground. The diameter of the cathode and the anode is 70 and 100 mm, respectively. The cathode−anode spacing was about 5 cm, and plasma glow discharge was produced in the zone between the cathode and the anode. Three Mo flakes one above the other were placed onto the Cu anode. From above to below, the diameter of the three Mo flakes is 40, 50, and 50 mm, respectively, and the carbon fiber substrate was placed onto the Mo flake with a diameter of 40 mm. The carbon fibers used in the experiment are polyvinyl alcohol (PVA)-based activated carbon fibers with a diameter range from 5 to 10 μm, which were purchased from Shanxi Institute of Coal Chemistry, Chinese Academy of Sciences. They were prepared from PVA fibers through the following steps: dehydration, heat-treatment, preoxidation, carbonization, and activation. The SEM image of carbon fibers is shown in the inset of Figure 3a.

Before the deposition of NCG films, carbon fibers were ultrasonically cleaned in deionized water, acetone, and ethanol for 5 min, respectively, and the surfaces were functionalized by immersion treatment in the solution of H_2SO_4/HNO_3 (1:3 v/v) for about 30 min. The bundles of carbon fibers were dispersed, and were laid onto the small Mo flake. Then the smaller Mo flake was carefully placed on the two larger Mo flakes, which were linked with the Cu anode. The reactor chamber was shut off, and then was pumped by a mechanical pump. When the chamber pressure was pumped out to below 6.0×10^{-2} Pa, H_2 gas with a flow rate of 300 sccm was introduced to produce glow discharge. The glow discharge was maintained, and the surface of carbon fibers was treated by hydrogen plasma for 30 min. Then CH_4 and Ar gases were introduced into the chamber, and the flow ratio of the $CH_4/Ar/H_2$ was controlled to be 10/70/30 sccm. The temperature of carbon fiber surfaces was adjusted by DC voltage, current, and chamber pressure, and was measured by an infrared temperature sensor. The infrared temperature sensor was fixed in front of the observation window and the lens was aimed at the carbon fibers, then the surface temperature of the carbon fibers was detected. When the DC voltage, current, and chamber pressure were 400 V, 3.1 A, and 6.3×10^3 Pa, respectively, the surface temperature of carbon fibers reached 973 K. Then the NCG films were deposited on the surfaces of carbon fibers, and the deposition time was about 0.5 and 2 h, respectively. Finally, the gas valves and the power supply were shut off, and the chamber pressure was pumped out to below 6×10^{-2} Pa.

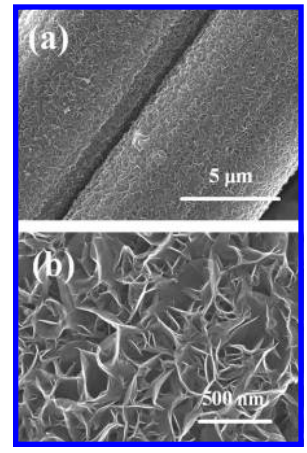

Figure 2. Low-resolution (a) and high-resolution (b) SEM images of NCG films grown on carbon fiber substrate for 0.5 h.

The morphology of the obtained products was characterized by scanning electron microscope (Hitachi S-4800) operated with an accelerating voltage of 20 kV. The microstructure was characterized by transmission and high-resolution transmission electron microscope (Tecnai F 30) operated with an accelerating voltage of 300 kV and Raman spectrometer (Renishaw inVia) at a laser wavelength of 514.5 nm from an Ar^+ laser.

3. Results and Discussion

Figure 2 shows the SEM images of NCG films grown on carbon fiber substrate for 30 min. As shown in Figure 2a, the surfaces of carbon fibers are covered by porous NCG films, and the diameters of carbon fibers are about 9 μm. In comparison with the diameter of pure carbon fibers shown in the inset of Figure 3a, it can be estimated that the thickness of NCG films grown on the surface of carbon fibers for 0.5 h is about 500 nm. In Figure 2b, it can be observed that the NCG thin film consists of petal-like graphite nanosheets. The sizes of nanosheets are about 300 nm and the thickness is below 20 nm, but the edge of nanosheets is very sharp.

Figure 3 shows the SEM images of NCG films grown on carbon fiber substrate for 2 h. As seen in the inset of Figure 3a, the diameters of pure carbon fibers are about 8 μm. However, after NCG films were grown on the surface of carbon fibers for 2 h, the diameters are increased to 40−60 μm as shown in Figure 3a. It can be estimated that the thickness of NCG films grown on the surface of carbon fibers for 2 h is about 15−25 μm. In Figure 3b, it can be observed that NCG films consist of clusters of petal-like graphite nanosheets. In panels c and d of Figure 3,

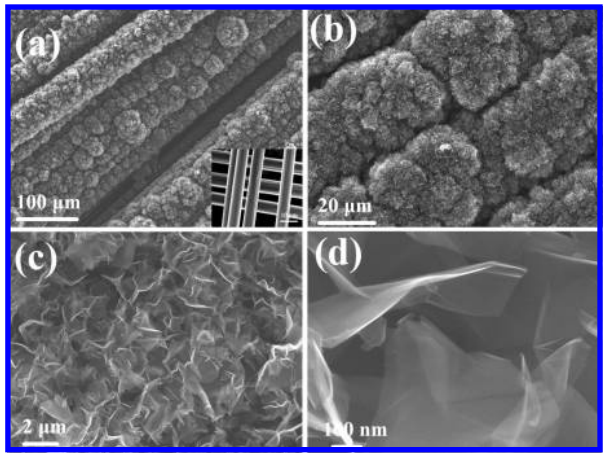

Figure 3. Low-resolution (a and b) and high-resolution (c and d) SEM images of NCG films grown on carbon fiber substrate for 2 h.

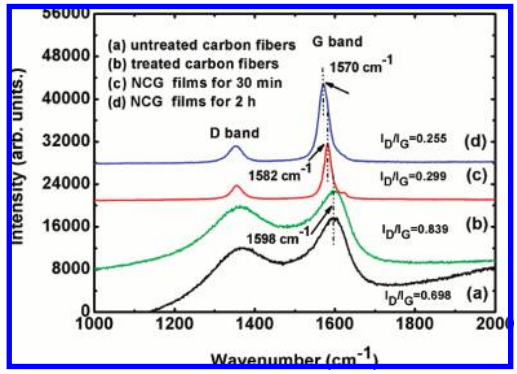

Figure 4. Raman spectra of untreated (a), treated carbon fibers (b), and NCG films grown on carbon fiber substrate for 0.5 (c) and 2 h (d).

the high-resolution SEM images of NCG films show that the sizes of nanosheets are about 1−2 μm, and the thickness is below 15 nm. In comparison with the NCG films grown on carbon fibers for 0.5 h, it can be concluded that the growth rate was slow at the initial deposition stage of NCG films, but the films can quickly grow after it is deposited for 0.5 h. Furthermore, along with the increase of deposition time, the sizes of graphite nanosheets get larger, but the thickness gets thinner. On the basis of the above results, the growth rates of NCG films can be estimated to be about 1 and 10 μm/h for the deposition time of 0.5 and 2 h, respectively. The difference of growth rates at different deposition stages of NCG films may be attributed to the nucleation and the growth of graphite nanosheets. At the initial stage of deposition, NCGs nucleated on the surface of carbon fibers, because the surface defects and functionalized groups of carbon fibers formed by the acid immersion and the hydrogen plasma treatment provided the growth sites of NCGs. At the second stage, NCGs can nucleate again, and then quickly grow on the NCG nucleation. The graphite nanosheets deposited at the initial stage provided considerable growth sites for the growth of NCG films.

The NCG films grown on carbon fibers have been analyzed by Raman spectroscopy. Figure 4 shows the typical Raman spectra of carbon fibers and NCG films grown on carbon fibers for 0.5 and 2 h, respectively. The G band at about 1570−1600 cm^{-1} corresponds to an E_{2g} mode of graphite, which is due to the sp^2-bonded carbon atoms in a two-dimensional hexagonal graphitic layer, and the D band at about 1350 cm^{-1} is associated with the presence of defects in the hexagonal graphitic layers, which are similar to the typical Raman spectra of CNTs.[27–31] Furthermore, the G band is accompanied by a weak shoulder peak at about 1620 cm^{-1}, which can be observed due to the breakdown of translational and local lattice symmetries of graphite. The 1620 cm^{-1} band is related to the presence of the crystalline edge, and is also associated with the presence of defects in the lattice and originates from a double resonance process involving $q \approx 2k$ phonons close to the Brillouin zone center.[32–34] As seen in Figure 4, two broad bands are present in the Raman spectra of untreated and treated carbon fibers. However, after NCG films are grown on carbon fibers, the D and G bands of Raman spectra become narrower and sharper due to the increase of graphite contribution to the products. Furthermore, the intensity ratio of the D peak to the G peak indicates the graphitization degree and purity of CNTs and graphite materials.[35] On the basis of the Raman spectra, the I_D/I_G of untreated and treated carbon fibers and NCG films grown on carbon fibers for 0.5 and 2 h can be estimated to be about 0.698, 0.839, 0.299, and 0.255, respectively. The difference of I_D/I_G ratio may be explained by the differences between different graphite material contributions. Before the deposition of NCG films, the carbon fibers were immersed in the solution of H_2SO_4/HNO_3, and were etched by hydrogen plasma. The immersion and etching treatment may increase the Raman I_D/I_G ratio of carbon fiber, which could be similar to that of CNTs.[36] Therefore, the immersion and etching treatment led to the surface defect of carbon fibers, which increased the I_D/I_G ratio. After the deposition of NCG films, the I_D/I_G ratio got small due to the increase of graphite material contribution. With the increase of deposition time, the I_D/I_G ratio got smaller, because more graphite structure was contained in the films. The results indicate that the graphitization degree and purity of NCG films on carbon fibers can be improved by increasing the deposition of NCG films.

In comparison with the Raman spectra labeled b, c, and d, it can be observed that the Raman frequency of the G peak is reduced by about 30 cm^{-1} from spectrum b to spectrum d. It is known that the G band is the characteristic peak of the graphite structure. The defect and impurity of graphite can change the I_D/I_G ratio, but cannot change the position of the G peak. In general, the characteristic Raman peak of nanomaterials can be shifted along with the temperature changes of sample surface, and the high temperature is responsible for the Raman shift to a higher frequency.[37] In our experiment, all the NCG films were prepared at the same temperature of 973 K, and the heat-treatment of NCG films was not carried out. The influence of the temperature effect on the Raman shift may be related to the laser radiation time of NCG films, when the Raman test was carried out. The long laser irradiation time could increase the surface temperature of samples, which may lead to the Raman shift toward higher frequency. Therefore, the surface temperature differences of NCG films heating by laser radiation were the reason that the Raman peak position of NCG films shifted to a lower frequency.

The microstructure of graphite nanosheets was characterized by TEM and HRTEM in Figure 5. As seen in Figure 5a, graphite nanosheets look like thin carbon paper, and the sizes of nanosheets are about 1 μm. Figure 5b shows the edge TEM image of graphite nanosheets. It can be seen that the edge is sharp and even curly. The selected area electron diffraction pattern of NCGs is shown in the inset of Figure 5b. Four diffraction rings, which correspond to the (002), (100), (102), and (100) planes of graphite with hexagonal structure, can be clearly observed. Panels c and d of Figure 5 show the HRTEM images of graphite nanosheets. As seen in Figure 5c, the

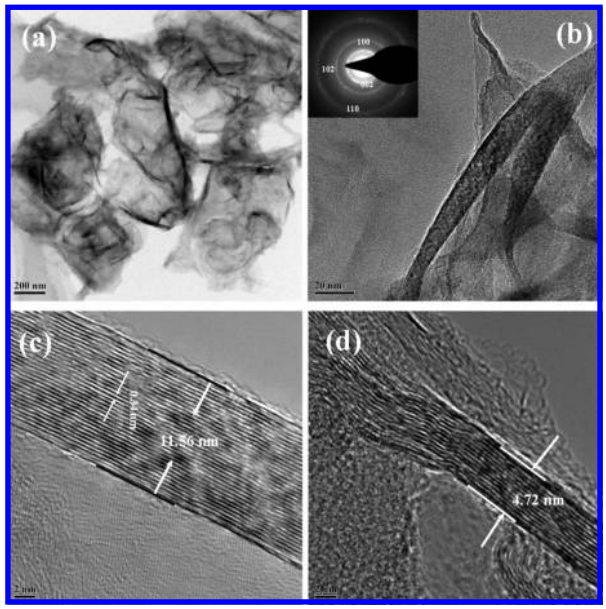

Figure 5. TEM (a and b) and HRTEM (c and d) images of NCG films.

thickness of the graphite nanosheet is about 11.56 nm, and the interplanar spacing is measured to be 0.34 nm, which is consistent with the (002) plane spacing of graphite. The number of graphite layers can be estimated to be about 34. Figure 5d shows that the thickness of the thin graphite nanosheet is about 4.72 nm, and the number of graphite layers is estimated to be about 14. The clear crystal plane images indicate the high purity and graphitization degree of NCG films.

Thus, SEM, TEM, HRTEM, and Raman data have shown that the films deposited by the DC-PCVD method on carbon fiber substrate have good crystalline graphite structure. However, in our previous work, using similar experimental conditions, nanocrystalline diamond (NCD) films were prepared on silicon substrate by the DC-PCVD method with $CH_4/Ar/H_2$ gas mixture, and the graphite impurity in NCD films was increased along with the increase of CH_4 concentration.[38] Although the higher CH_4 concentration and lower growth temperature are favorable for the formation of graphite structure, they are not sufficient for the growth of only NCG films with the experimental conditions of the $CH_4/Ar/H_2$ composition of 10/70/30 sccm and the substrate temperature of 973 K, which are still within a scope of the growth condition of NCD films. Therefore, carbon fiber substrate should be responsible for the deposition of graphite nanosheets. Taking into account the substrate species of carbon fibers, we can propose a formation mechanism of graphite nanosheets on carbon fiber substrate. First, the treatment of carbon fibers in the solution of H_2SO_4/HNO_3 destroyed partly the surface structure and increased the functionalized bonds of −COOH on the surface of carbon fibers, which may provide the growth sites of graphite nanosheets.[39] Then the hydrogen plasma treatment increased the functionalized bonds of C−H and further improved the surface activity of carbon fibers, which should be similar to the result of CNTs treated by hydrogen plasma.[36] Finally, CH_4 gas was introduced into the reactor chamber and formed C_2 radicals in the plasma. These C_2 radicals were absorbed on the surface of carbon fibers, and formed amorphous carbon and hexagonal graphite structure.[21] At the beginning stage of deposition, both amorphous carbon and graphite nanosheets were grown due to the finite growth sites of graphite nanosheets on the surface of carbon fibers, and the nucleation process of nanosheets on carbon fibers led to the low growth rate. After the surface of carbon fibers was covered by graphite nanosheets, the secondary nucleation occurred on the surface of nanosheets, and then the NCG films were grown with high growth rate. Therefore, the substrate species and the treatment of carbon fibers are favorable for the deposition of NCG films.

4. Conclusion

We synthesized NCG films on carbon fibers by the DC-PCVD method. The sizes of graphite nanosheets were about 0.3 to 2 μm, and the thickness of nanosheets ranged from 5 to 20 nm. The growth rate of films increased, and the purity and graphitization degree of NCG films can be improved by increasing the deposition time of graphite nanosheets. In comparison with the products grown on silicon substrate under similar experimental conditions, the substrate species and the treatment of carbon fibers were responsible for the growth of graphite nanosheets. The carbon fibers/NCG film composites could have potential applications in electrochemistry and nanoelectronic fields, and so forth.

Acknowledgment. This work was supported by the National Natural Science Foundation of China (NSFC, Grant Nos. 50072029 and 50572101) and the tackle hard-nut program in science and technology of Heilongjiang Province of China (Grant No. 2006G2016-00). Furthermore, the authors would also like to thank Dr. Zhu Ruihua for the help of the SEM test.

References and Notes

(1) Jishi, R. A.; Dresselhaus, G. *Phys. Rev. B* **1982**, *26*, 4514.
(2) Hass, K. C. *Phys. Rev. B* **1992**, *46*, 139.
(3) Bunch, J. S.; Yaish, Y.; Brink, M.; Bolotin, K.; McEuen, P. L. *Nano. Lett.* **2005**, *5*, 287.
(4) Zhang, Y.; Small, J. P.; Pontius, W. V.; Kim, P. *Appl. Phys. Lett.* **2005**, *86*, 073104.
(5) Berger, C.; Song, Z.; Li, T.; Li, X.; Ogbazghi, A. O.; Feng, R.; Dai, Z. T.; Marchenkov, A. N.; Conrad, E. H.; First, P. N.; de Heer, W. A. *J. Phys. Chem. B* **2004**, *108*, 19912.
(6) Rinzler, A. G.; Hafner, J. H.; Nikolaev, P.; Lou, L.; Kim, S. G.; Tomanek, D.; Nordlander, P.; Colbert, D. T.; Smalley, R. E. *Science* **1995**, *269*, 1550.
(7) de Heer, W. A.; Chatelain, A.; Ugarte, D. A. *Science* **1995**, *270*, 1179.
(8) Obraztsov, A. N.; Zakhidov, A. A.; Volkov, A. P.; Lyashenko, D. A. *Diamond Relat. Mater.* **2003**, *12*, 446.
(9) Wang, J. Y.; Ito, T. *Diamond Relat. Mater.* **2007**, *16*, 589.
(10) Nakada, K.; Fujita, M.; Dresselhaus, G.; Dresselhaus, M. S. *Phys. Rev. B* **1996**, *54*, 17954.
(11) Wakabayashi, K.; Fujita, M.; Ajiki, H.; Sigrist, M. *Phys. Rev. B* **1999**, *59*, 8271.
(12) Gonzalez, J.; Guinea, F.; Vozmediano, M. A. H. *Phys. Rev. B* **2001**, *63*, 134421.
(13) Bunch, J. S.; van der Zande, A. M.; Verbridge, S. S.; Frank, I. W.; Tanenbaum, D. M.; Parpia, J. M.; Craighead, H. G.; McEuen, P. L. *Science* **2007**, *315*, 490.
(14) Hill, E. W.; Geim, A. K.; Novoselov, K.; Schedin, F.; Blake, P. *IEEE Trans. Magn.* **2006**, *42*, 2694.
(15) Zhu, M. Y.; Wang, J. J.; Outlaw, R. A.; Hou, K.; Manos, D. M.; Hollowav, B. C. *Diamond Relat. Mater.* **2007**, *16*, 196.
(16) Wang, J. J.; Zhu, M. Y.; Outlaw, R. A.; Zhao, X.; Manos, D. M.; Hollowav, B. C. *Carbon* **2004**, *42*, 2867.
(17) Shang, N. G.; Au, F. C. K.; Meng, X. M.; Lee, C. S.; Bello, I.; Lee, S. T. *Chem. Phys. Lett.* **2002**, *358*, 187.
(18) Wang, J. J.; Zhu, M. Y.; Outlaw, R. A.; Zhao, X.; Manos, D. M.; Holloway, B. C.; Mammana, V. P. *Appl. Phys. Lett.* **2004**, *85*, 1265.
(19) Hiramatsu, M.; Shiji, K.; Amano, H.; Hori, M. *Appl. Phys. Lett.* **2004**, *84*, 4708.
(20) Wu, Y. H.; Qiao, P. W.; Chong, T. C.; Shen, Z. X. *Adv. Mater.* **2002**, *14*, 64.
(21) Obraztsov, A. N.; Obraztsova, E. A.; Tyurnina, A. V.; Zolotukhin, A. A. *Carbon* **2007**, *45*, 2017.
(22) Zeng, L. Y.; Lei, D.; Wang, W. B.; Liang, J. Q.; Wang, Z. Q.; Yao, N.; Zhang, B. L. *Appl. Surf. Sci.* **2008**, *254*, 1700.

(23) Zeng, L. Y.; Wang, W. B.; Lei, D.; Liang, J. Q.; Xia, Y. X.; Zhao, H. F.; Kong, X. G.; Zhao, J. L. *Carbon* **2008**, *46*, 359.

(24) Meinke, O.; Kaempfer, D.; Weickmann, H.; Friedrich, C.; Vathaner, M.; Warth, H. *Polymer* **2004**, *45*, 739.

(25) Tang, W.; Santare, M. H.; Advani, S. G. *Carbon* **2003**, *41*, 2779.

(26) Thostenson, E. T.; Li, W. Z.; Wang, D. Z.; Ren, Z. F.; Chou, T. W. *J. Appl. Phys.* **2002**, *91*, 6034.

(27) Tuinstra, F.; Koenig, J. *J. Chem. Phys.* **1970**, *53*, 1126.

(28) Reznik, D.; Olk, C. H.; Neumann, D. A.; Copley, J. R. D. *Phys. Rev. B* **1995**, *52*, 116.

(29) Shanmugam, S.; Gedanken, A. *J. Phys. Chem. B* **2006**, *110*, 2037.

(30) Nemanich, R. J.; Solin, S. A. *Phys. Rev. B* **1979**, *20*, 392.

(31) Yu, J.; Zhang, Q.; Ahn, J.; Yoon, S. F.; Rusli;Li, Y. J.; Gan, B.; Chew, K.; Tan, K. H. *Diamond Relat. Mater.* **2001**, *10*, 2157.

(32) Yasushi, K.; Gen, K. *Phys. Rev. B* **1995**, *52*, 10053.

(33) Saito, R.; Jorio, A.; Souza Filho, A. G.; Dresselhaus, G.; Dresselhaus, M. S.; Pimenta, M. A. *Phys. Rev. Lett.* **2002**, *88*, 027401.

(34) Tan, P. H.; Hu, C. Y.; Dong, J.; Shen, W.; Zhang, B. *Phys. Rev. B* **2001**, *64*, 214301.

(35) He, C.; Zhao, N.; Shi, C.; Du, X.; Li, J.; Cui, L. *J. Alloys Compd.* **2006**, *425*, 329.

(36) Zeng, L. Y.; Wang, W. B.; Liang, J. Q.; Wang, Z. Q.; Xia, Y. X.; Lei, D.; Ren, X. G.; Yao, N.; Zhang, B. L. *Mater. Chem. Phys.* **2008**, *108*, 82.

(37) Wang, D.; Chen, B.; Zhao, J. *J. Appl. Phys.* **2007**, *101*, 113501.

(38) Zeng, L. Y.; Peng, H. Y.; Wang, W. B.; Chen, Y. Q.; Lei, D.; Qi, W. T.; Liang, J. Q.; Zhao, J. L.; Kong, X. G.; Zhang, H. *J. Phys. Chem.C* **2008**, *112*, 1401.

(39) Zhang, G.; Sun, S.; Yang, D.; Dodelet, J.; Sacher, E. *Carbon* **2008**, *46*, 196.

JP801615W